

# A Bayesian Filtering Approach with Time-Frequency Representation for Corrupted Dual Tone Multi Frequency Identification

Nattapol Aunsri, *Member, IAENG*

**Abstract**—This paper addresses the identification of the Dual Tone Multiple Frequency (DTMF) signal from real environments where the signal was corrupted during acquisition and transmission processes by using the sequential Bayesian filtering along with the time-frequency representation of time-series. The mathematical and statistical models were employed to estimate the frequency content embedded in the real DTMF signal. A sequential state-space framework, by treating each frequency component as a target to be tracked, that is developed in this work for the extraction of time-frequency information from time slice spectrograms provides excellent results, stemming from an efficient representation of the DTMF signals in the frequency domain. The paper also illustrates the accuracy of the estimates by displaying the probability density functions (PDFs) of the frequencies obtained from the filter. The performance of the proposed approach was compared to those of the conventional method. The comparison demonstrates a significant benefit of our method for DTMF signal identification under various noisy environments.

**Index Terms**—Dual Tone Multiple Frequency, sequential Bayesian filtering, particle filter (PF), frequency estimation, time-frequency, signal processing.

## I. INTRODUCTION

The telephone network is designed to carry the voice signals. To make a phone call with the touch tone phones, it is traditionally performed over the keypads. DTMF has long been used as the signalling system for identifying the keys or actually the numbers that the caller is dialling. Besides, the DTMF is also used in data transmission over the air amateur radio frequency bands. Many applications that require interactive control, telephone banking, ATM machines, for examples, utilize the DTMF signaling. Each DTMF signal is composed of a pair of two different sinusoidal signals (tones). Each pair of such tones represents a unique number or a symbol and this representation is the international standard used globally. To illustrate, for example, if the key ‘1’ is pressed, the DTMF signal with the designated frequencies of 697 Hz and 1,209 Hz is generated, which is sent out for processing. Table 1 summarizes the DTMF frequencies.

The DTMF tones may be generated either mathematically or from a look-up table. By means of Digital Signal Processing, the digital samples of two sine waves are generated mathematically, then scaled, and added together. At the receiver, the logarithmically-compressed, 8-bit digital data words from the codec are received and logarithmically expanded to their 16-bit linear format. Then, the tones are

detected to decide on the transmitted digit. Traditionally, the DFT implementation via fast Fourier Transform (FFT) is used as a detection tool. Since each DTMF signal is composed of a pair of tones, the filter bank is typically more efficient.

In the real environment where the transmission channel and interference cannot be simply considered as just linear and additive Gaussian, the classical filtering methods generally fail to accomplish their mission [1]. More sophisticated framework, where the simple assumption is relaxed, must be used for the filtering method.

A probabilistic framework is often considered as the optimal way to perform tracking in order to deal with uncertainty over time. Since tracking DTMF signals that are evolving with time is the goal of this work, such a framework is suitable. This work builds on Bayesian filtering approach for tracking time-varying spectral features of DTMF signal. The technique incorporates a state equation that determines how frequency evolves at each time step, and an observation equation, that is used in likelihood formulation based on observed data. The mathematical and statistical foundations of Bayesian filtering have been extensively presented in the literature. The very first filter that was proposed is the well-known Kalman Filter (KF) [2], that estimated the parameters in cases of additive and Gaussian perturbations in the evolution of the unknown parameters, additive Gaussian noise present in the measured data, and a linear relationship between measurements and state vector parameters.

As just mentioned above, KFs are the foundations of sequential Bayesian filtering. When (a) consecutive state parameters vary linearly, (b) data and parameters are linearly related, and (c) noise both in the state and observation equations is additive and Gaussian, the KF is the optimal estimator for parameters between the consecutive steps in the sense that the root mean squared (RMS) errors are minimized. Hence, the classical KF has been extensively and successfully employed for the solution of many problems under linear and Gaussian assumptions. Based on the linearity and Gaussian nature of the noise, the KF delivers PDFs of the state parameters by propagating their expectations and covariances from state to state. In other words, the expectations and covariances of the state parameters from previous time step are used for the next time step.

When the problem encounters nonlinear/non-Gaussian systems as well as non-additive noise, variations or generalizations of the standard filter are necessary. Subsequent developments of the KFs were announced to solve those problems such as EKFs, UKFs. A series of these filters can be, for examples, found in [3], [4], [5], [6], [7]. Nevertheless,

Manuscript received March 30, 2016; revised August 10, 2016.

N. Aunsri is with the School of Information Technology, Mae Fah Luang University, Chiang Rai, 57100, Thailand, e-mail: nattapol.aun@mfu.ac.th, http://itschool.mfu.ac.th/).

strongly nonlinear models and complex noise processes require numerical methods for the computation of posterior PDFs and, ultimately, point estimates and uncertainty. A recent and powerful method for nonlinear/non-Gaussian filtering developed for such circumstances is particle filtering. It is a class of Monte Carlo simulation-based and recursive Bayesian framework filtering methods for nonlinear/non-Gaussian systems, a system setting where conventional methods often fail to achieve satisfactory estimation. Particle filtering framework is based on random point-mass representations of the state parameters PDFs, which captures the time-varying characteristics of the states. Some problems that particle filtering has been encountered are given in [8], [9], [10].

The rest of the paper is organized as follows. Sect. II presents the foundations of sequential Bayesian filtering framework and the particle filtering formulation. Sect. III discusses the time-frequency model that is employed for describing the spectrogram slices of the DTMF signal for this work. Sect. IV provides how the time-frequency model and particle filter (PF) can be combined to track recorded DTMF signals in various environments. Conclusions can be found in Sect. V.

TABLE I  
DTMF KEY FREQUENCIES

Frequencies	1209 Hz	1336 Hz	1477 Hz	1633 Hz
697 Hz	1	2	3	A
770 Hz	4	5	6	B
852 Hz	7	8	9	C
941 Hz	*	0	#	D

## II. BAYESIAN FILTERING

### A. State Space Model

In order to analyse and make any inference about a dynamic system, two following models are needed. A transition model that describes the evolution of the state with time or space depending on the task at hand, and an observation model that relates noisy data measurements to the state vector. Both models can be written, respectively, as:

$$\mathbf{X}_n = \mathbf{F}_{n-1}(\mathbf{X}_{n-1}, \mathbf{V}_{n-1}) \quad (1)$$

$$\mathbf{Y}_n = \mathbf{G}_n(\mathbf{X}_n, \mathbf{W}_n). \quad (2)$$

The Equation (1) is the state or system equation describing the evolution or transition of  $\mathbf{X}_n$  that is followed the first order Markov process. Function  $\mathbf{F}_n$  is a known function relating the state vector at step  $n$  to that at step  $n - 1$ . In addition, term  $\mathbf{V}_n$  represents the state noise or perturbation from one state to the next and has a known probability density function (PDF).

Another Equation is the observation equation that relates the measurements  $\mathbf{Y}_n$  to the state vector  $\mathbf{X}_n$  through function  $\mathbf{G}_n$ , which actually is the mathematical description via the physical model of the problem. In most problems, the function  $\mathbf{G}_n$  is a known function, but for some scenarios it can be unknown function and is estimated at the preprocessing step. Finally, the term  $\mathbf{W}_n$  is the measurement/observation noise and typically known.

### B. Bayesian Inference

Let  $\mathbf{X}_n = [\mathbf{x}_1, \mathbf{x}_2, \dots, \mathbf{x}_n]$  be the sequence of the unknown state vectors and  $\mathbf{Y}_n = [\mathbf{y}_1, \mathbf{y}_2, \dots, \mathbf{y}_n]$  be the set of the observations measured at the first  $n$  steps. With the prior density  $p(\mathbf{X}_0)$ , the posterior PDF,  $p(\mathbf{X}_n|\mathbf{Y}_n)$ , can be written as:

$$p(\mathbf{X}_n|\mathbf{Y}_n) = \frac{p(\mathbf{Y}_n|\mathbf{X}_n)p(\mathbf{X}_0)}{p(\mathbf{Y}_n)}. \quad (3)$$

The posterior PDF (3) contains all information about the state  $\mathbf{X}_n$  that is hidden in the observation data  $\mathbf{Y}_n$ . Given  $\mathbf{X}_n$ , assume that the observation data up to step  $n$  are independent; and conditional on  $\mathbf{x}_n$ , the observation  $\mathbf{y}_n$  is independent of the states at all other times. Therefore, the likelihood can be expressed by

$$p(\mathbf{Y}_n|\mathbf{X}_n) = \prod_{i=1}^n p(\mathbf{y}_i|\mathbf{x}_i). \quad (4)$$

Since the first order Markov process is assumed here, we can write (3) as:

$$p(\mathbf{X}_n|\mathbf{Y}_n) = \frac{p(\mathbf{x}_0) \prod_{i=1}^n p(\mathbf{y}_i|\mathbf{x}_i)p(\mathbf{x}_i|\mathbf{x}_{i-1})}{p(\mathbf{Y}_n)}. \quad (5)$$

The efficient Bayesian framework recursively estimates the marginal PDF  $p(\mathbf{x}_n|\mathbf{Y}_n)$  from  $p(\mathbf{x}_{n-1}|\mathbf{Y}_n)$ . The process is explained here. Let the marginal PDF  $p(\mathbf{x}_{n-1}|\mathbf{Y}_{n-1})$  is available, the prediction of the  $p(\mathbf{x}_n|\mathbf{Y}_{n-1})$  can be calculated from the transitional PDF  $p(\mathbf{x}_n|\mathbf{x}_{n-1})$ . The transitional density is obtained from the system equation and the state noise PDF. Under the first order Markov chain assumption, the PDF  $p(\mathbf{x}_n|\mathbf{Y}_{n-1})$  can be expressed as the so called Chapman-Kolmogorov equation:

$$\begin{aligned} p(\mathbf{x}_n|\mathbf{Y}_{n-1}) &= \int p(\mathbf{x}_n|\mathbf{x}_{n-1}, \mathbf{Y}_{n-1})p(\mathbf{x}_{n-1}|\mathbf{Y}_{n-1})d\mathbf{x}_{n-1} \\ &= \int p(\mathbf{x}_n|\mathbf{x}_{n-1})p(\mathbf{x}_{n-1}|\mathbf{Y}_{n-1})d\mathbf{x}_{n-1}. \end{aligned} \quad (6)$$

According to the Bayes theorem, the new estimate of the state vector at step  $n$  is:

$$p(\mathbf{x}_n|\mathbf{Y}_n) = \frac{p(\mathbf{y}_n|\mathbf{x}_n)p(\mathbf{x}_n|\mathbf{Y}_{n-1})}{p(\mathbf{y}_n|\mathbf{Y}_{n-1})}. \quad (7)$$

Given that the observation data  $\mathbf{Y}_n$  is available, the likelihood of the state vector  $\mathbf{x}_n$  is obtained from the density  $p(\mathbf{y}_n|\mathbf{x}_n)$ . Fig. 1 shows the sequential update from stem  $n - 1$  to step  $n$ .

Since the posterior PDF of the states is available from the sequential update described above, the interference can be performed using this distribution. The estimate function of the state can now be computed from

$$\begin{aligned} \widehat{F(\mathbf{x}_n)} &= \mathbf{E}_{p(\mathbf{x}_n|\mathbf{Y}_n)}[F(\mathbf{x}_n)|\mathbf{Y}_n] \\ &= \int F(\mathbf{x}_n)p(\mathbf{x}_n|\mathbf{Y}_n)d\mathbf{x}_n. \end{aligned} \quad (8)$$

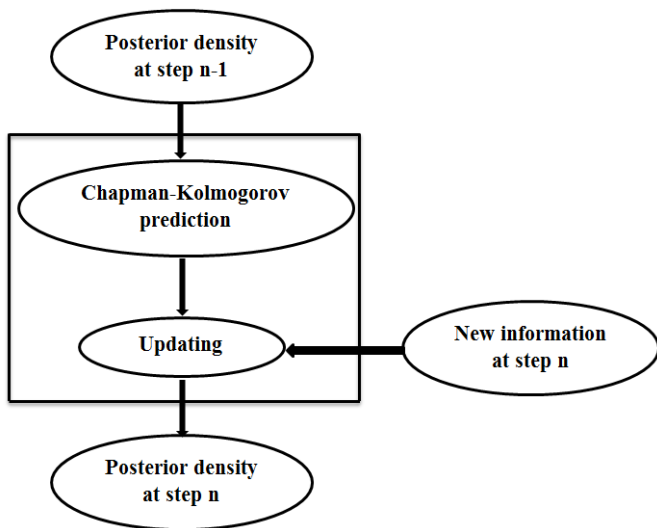


Fig. 1. A sequential update of the posterior density from step  $n - 1$  to step  $n$ .

### C. Particle Filters

Particle filtering performs sequential estimation based on representation of probability densities of which main characteristics (mean and variance, for example) are not known. The idea is that the posterior density is represented by a set of particles, and their associated weights which correspond to probabilities,  $\{\mathbf{x}_n^i, w_n^i\}_{i=1}^N$ , where  $N$  is the number of particles. In other words, we can approximate the PDF by the point-mass histogram from the random sampling of the state space.

Particle filtering utilizes the sequential updating as described above. This work uses sequential importance sampling (SIS) [11] to estimate the conditional density of the state given past observations in the PF implementation. The idea of the SIS is that the output of the previous step forms the prior for the next one. For each time step, the approximated density  $p(\mathbf{x}_n|\mathbf{y}_n)$  is given by

$$p(\mathbf{x}_n|\mathbf{y}_n) = \sum_{i=1}^N w_n^i \delta(\mathbf{x}_n - \mathbf{x}_n^i) \quad (9)$$

and

$$w_n^i \propto \frac{p(\mathbf{X}_n^i|\mathbf{Y}_n)}{q(\mathbf{X}_n^i|\mathbf{Y}_n)}, \quad (10)$$

where  $\delta$  is the Dirac delta function, and  $N$  is the number of particles used in the approximation and this quantity dictates the accuracy of the filter [1], [12]. The quantity  $q(\mathbf{X}_n^i|\mathbf{Y}_n)$  is the importance density. If the results from the previous time step are used and the importance density is chosen as

$$q(\mathbf{X}_n|\mathbf{Y}_n) = q(\mathbf{x}_n|\mathbf{X}_{n-1}, \mathbf{Y}_n)q(\mathbf{x}_{n-1}, \mathbf{Y}_{n-1}), \quad (11)$$

we can write the posterior PDF as:

$$p(\mathbf{X}_n|\mathbf{Y}_n) = \frac{p(\mathbf{y}_n|\mathbf{x}_n)p(\mathbf{x}_n|\mathbf{x}_{n-1})}{p(\mathbf{y}_n|\mathbf{Y}_{n-1})}p(\mathbf{X}_{n-1}, \mathbf{Y}_{n-1}). \quad (12)$$

By substituting (11) and (12) into (10) and as suggested by [12], [13] for the choice of the proposal density to minimize

the IS error, the weight of the  $i$ th particle can then be simply written as (for the full details, please see [12])

$$w_n^i = p(\mathbf{y}_n|\mathbf{x}_n^i)w_{n-1}^i. \quad (13)$$

The variance of the importance weights increases with time [1], [12], [14]. This strongly influences the filter performance since the majority of the normalized weights tends to be zero after a few states. This is called the degeneracy problem. Implementation of suitable methods is necessary for resolving this problem; this leads to the resampling scheme. The recent work that makes use of the resampling scheme has been reported in [15]. Resampling is a key process for the successful implementation of PFs. The resampling procedure is used to generate multiple copies of those particles with significant weights and remove those particles with negligible importance weights. The particles with larger weights may be chosen a number of times and samples with small weights may not be selected at all. After resampling process, the offspring particles are centralized around the parameters that are of interest. The process that includes resampling within sequential filtering is referred to as Sequential Importance Resampling (SIR) [13], [16]. A technique for deciding the need for resampling is to use the effective number of particles needed to avoid the degeneracy problem by comparing to the threshold defined by:

$$N^{eff} = \frac{1}{\sum_{i=1}^N (w_n^i)^2}. \quad (14)$$

Although one can reduce the effect of degeneracy through the resampling process, a problem that could occur is the loss of particle diversity. This is known as sample impoverishment and occurs when all particles are identical (all weights are equal). This is especially prevalent when the noise level in the measured data is very low. There are developments of the PFs [17], [18] that have been designed for remedying these problems. The algorithm called a diversity enhanced particle filter was proposed to improve the estimation accuracy. It is done by generating a new set of secondary particles from the very high weight primary particles and then combine those sets to construct the updated particles [19].

### III. PARTICLE FILTERING FOR TIME-FREQUENCY MODELLING OF DTMF SIGNALS

We consider each DTMF signal as

$$s(t) = \sum_{k=1}^2 A_k \sin(2\pi f_k t + \varphi_k), \quad (15)$$

where  $A_k$  is the amplitude,  $f_k$  is the frequency, and  $\varphi_k$  represents the phase of the  $k$ th component. Since each DTMF signal is composed of two tones, we therefore have two sinusoidal components appeared in (15). Extension of (15) can be easily used to model the multiple DTMF signals that were measured at the receiver; we will relax this for now without loss of generality. The spectrogram of the DTMF signal  $s(t)$  is obtained through the Short-Time Fourier Transforms (STFTs) and the corresponding squared magnitude of its STFT is obtained by:

$$SG_s = \frac{1}{2\pi} \left| \int s(\lambda)w(\lambda - t)e^{-j\omega\lambda}d\lambda \right|^2, \quad (16)$$

where  $w(t)$  is the window function used for enhancing the signal information in calculating the STFT.

We consider the measurement data via the transformed (frequency) domain because the frequency contents of the signal can be seen from it better than working in time-domain. Moreover, the expected number of the frequencies (number of tones) at a given time should be two or none, which is actually from the nature of the signal. From this setting, the Fourier transforms of the received data  $\mathbf{y}_n$  is ideally considered as the sum of the impulses in the frequency domain. For the real signal, the ideal conditions may not apply, the STFT of the received signal can be considered as the sum of the squared sinc function as analysed and reported in [20]. This leads us to the formulation of the measurement equation as

$$\mathbf{y}_n = \sum_{j=1}^2 A_{nj} z(f - x_{nj}) + \mathbf{w}_n. \quad (17)$$

The quantity  $\mathbf{y}_n$  is the spectrogram slice at time step  $n$ ,  $\mathbf{w}_n$  is assumed to be additive Gaussian noise in the spectrogram with the distribution  $\mathbf{w} \sim \mathcal{N}(\mathbf{0}, \sigma_w^2)$ , and  $z(\cdot)$  is the squared sinc function where its center is located at  $x_{nj}$ .

For the PF framework, the state and measurement equations for DTMF tracking are given as:

$$\mathbf{f}_n = \mathbf{f}_{n-1} + \mathbf{v}_n, \quad (18)$$

$$\mathbf{y}_n = \mathbf{G}(\mathbf{f}_n) + \mathbf{w}_n, \quad (19)$$

where  $\mathbf{f}_n$  is the vector containing frequencies of the DTMF signal. Quantities  $\mathbf{v}_n$  and  $\mathbf{w}_n$  are state and measurement noises and  $\mathbf{G}_n$  is the transmission channel. For the PF state equation (18), the state vector is composed of the frequencies. We simply consider that the DTMF is corrupted by the additive white Gaussian noise; with this assumption, as discussed in Sect. IV, the filtering results are excellent.

Not only the frequencies that we estimate via PF in this work, but also the corresponding amplitudes. In general, amplitudes are the elements in the state vector, we can treat them as the parameters to be estimated exactly the same as the frequencies. But by doing that we need to double the size of the state vector and this could degrade the computational performance. The alternative approach discussed in [20], [21], a maximum likelihood (ML) or a maximum a posteriori (MAP) estimator can be used for amplitudes estimation rather than a sampling procedure at each state. This could be done based on the assumption that the noise in the measurement is considered to be additive and Gaussian. Therefore, the conditional PDFs of the amplitudes on the frequencies can be found to be Gaussian. When the density function of the random variable is known, drawing samples from such distribution is possible. Since ML or MAP provides the means, and the covariance matrix of these conditional probability densities can be computed as well, constructing conditional PDFs of the amplitudes on frequencies is available. Drawing samples from these conditional PDFs forms the marginal posterior PDFs of the amplitudes at each time step. The obtained PDFs are used at the next time step for the prediction of the new set of frequencies at the next arrival time and, consequently, of corresponding amplitudes.

The multiple model particle filter (MMPF) [5], [12] is required in this work in order to estimate number of tones (frequencies) that is present at a given time. In other words, the filter incorporates the birth (appearance of new frequencies in the spectrogram) and death (disappearance of the existing frequencies in the spectrogram) processes in the estimating procedure. The dimension of  $\mathbf{f}_n$  in equation (18) is  $r_n$ , where  $r_n$  is the number of tones at time step  $n$ . Number of tones present at a given time could be 'two' or 'none.' This stems from the fact that when the touch-tone button is pressed at a specific time, two tones are presented. If the button is released, no tone should appear. However, we include the possibility of having one tone into the estimation process allowing the PF to smoothly change the number of tones from the previous step. In a noisy environment, the PF favors the model with the highest order because there is an inherent bias towards large dimensionality. To compensate for this, a penalizing factor is multiplied to the original likelihood for remedying the typical preference of the high-order models. This penalty factor comes from the prior density on the order. In this work, the prior densities are selected to be uniform:

$$p(A_{nj}) = \max(\mathbf{y}_n) \quad (20)$$

for each amplitude, and

$$p(x_{nj}) = \frac{1}{L} \quad (21)$$

for each tone, where  $L$  is the length of the Fourier transform that supports the frequency space. The likelihood function in this case is given by

$$p(\mathbf{y}_n | \mathbf{x}_n) \propto \frac{1}{L^{r_n}} \exp\left\{-\frac{1}{2\sigma_w^2} \|\mathbf{y}_n - \sum_{j=1}^{r_n} A_{nj} z(f - x_{nj})\|^2\right\}. \quad (22)$$

As discussed in Sect. II-C that SIR PF contains three steps where the prediction and update steps are two of the three of its building blocks. In this work, frequencies, amplitudes, model order (number of tones), and noise variance (considered as a nuisance parameter) are predicted using the samples from the previous time step and are updated based on how they fit in the PDF calculation, given the new data entering in the current time step. Prediction step utilizes the transition equation defined by (18) while the update step is done via the likelihood function expressed as in (22). SIR scheme, the third step for generating a set of efficient particles, is used after the update step for the next arrival time.

#### IV. TRACKING RESULTS

We first evaluate the filter performance from the tracks of the DTMF signal recorded from the automatic or modem dialling. This kind of DTMF signal is considered to be the cleanest signal and, therefore, the information is expected to be extracted from it easily. The spectrogram of the signal obtained via STFT calculation is shown in Fig. 2(a). The MAP estimates of the frequencies obtained from the PDFs calculated by the PF are shown in Fig. 2(b) with dots that are superimposed on the spectrogram. The number of particles used in this case was 100. PF tracks the frequencies of the DTMF signal greatly.

We now illustrate how the PF exhibits the PMF of the model order or the number of tones present at a given time

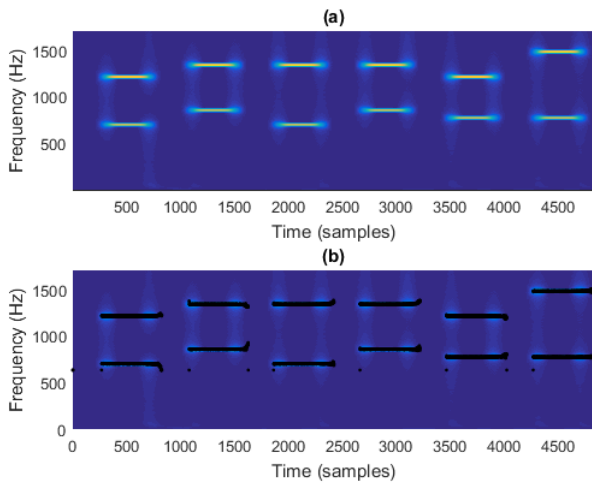


Fig. 2. (a) The spectrogram of the modem DTMF signal. (b) Frequency estimates of the signal superimposed on the spectrogram.

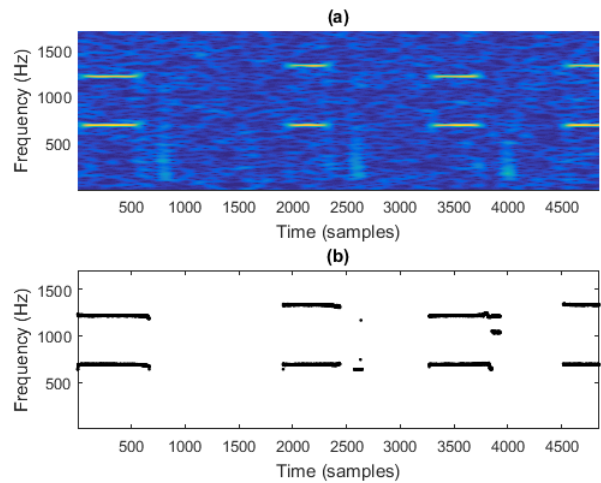


Fig. 4. (a) The spectrogram of the hand-dialled DTMF signal recorded over the network. (b) Frequency estimates of the signal.

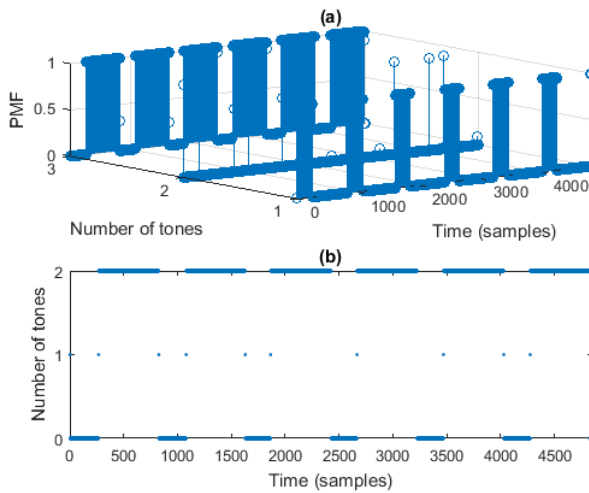


Fig. 3. Tracks of the modem DTMF signal. (a) PMF of the number of tones. (b) Number of tones estimates.

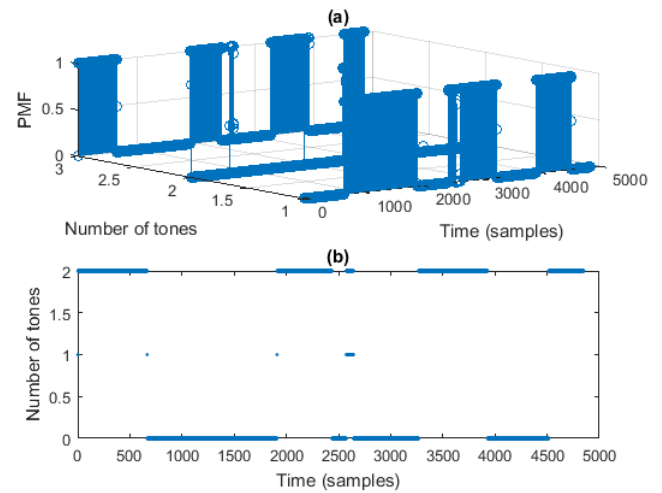


Fig. 5. Tracks of the hand-dialled DTMF signal recorded over the network. (a) PMF of the number of tones. (b) Number of tones estimates.

in Fig. 3(a) and the estimates number of tones in Fig. 3(b). From the results, The filter provides the PMF of the number of tones appearing in the signal as shown in Fig. 3(a) without significant error. This is as what was expected since the signal does not contain noise (from the nature when the signal was acquired) or just very low amount if it is present.

We apply our method to the hand-dialled DTMF signal recorded over the network. This scenario is very practical since we mostly transmit the signal through the networks, therefore the transmission channel can be disturbed by noise. Moreover, we do not assume here that the noise followed Gaussian distribution. Number of particles used in getting the results in this case was 200. Fig. 4(a) shows the spectrogram of the noisy DTMF signal as mentioned above. The frequency estimates by our PF are provided in Fig. 4(b). PMF of the number of tones and order estimates of this signal are presented in Fig. 5(a) and (b), respectively. As seen from the resulting estimates with the filter that they are very good, only few erroneous estimates are present.

To further investigate the performance of our model, we demonstrate in Fig. 6(a) the frequency estimates superimposed on the spectrogram; and the order estimates of

the wideband coupling, recorded locally, DTMF signal are presented in Fig. 6(b). The tracking results are excellent even the DTMF signal was corrupted by noise and transmitting media. Again, we used 200 particles in the tracking process.

Fig. 7 shows the results of the frequency estimates for the scenario that the hand-dialled DTMF signal recorded locally is considered; while Fig. 8 presents the PMF of the number of tones and order estimates of this signal, where in this case 150 particles was used in the process. Next, we show the validity of our model by demonstrating how close the estimates obtained from the PF to the received noisy DTMF signal. In Fig. 9, we show by solid line a slice of the spectrogram of the hand-dialled DTMF signal at times step 500 and the corresponding spectrum estimates from the PF (with 'diamond'). Although there is quite substantial noise level in the measured data, the match of the two DTMF frequencies from both spectrums is still excellent as obviously seen that the MAP spectrum almost coincides with the informative part of the data spectrum.

In addition to the estimates provided in Figs. 7-9. The PDFs estimated with the PF for the two frequencies at times step 150 are displayed in Figs. 10(a) and 10(b). The MAP

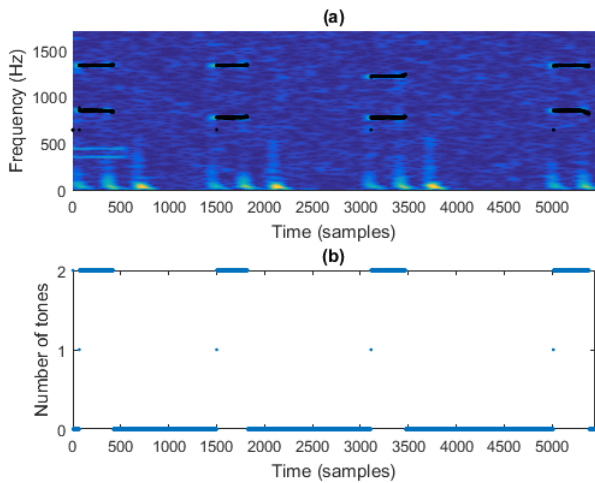


Fig. 6. Tracks of the wideband coupling, recorded locally, DTMF signal. (a) Frequency estimates. (b) Number of tones estimates.

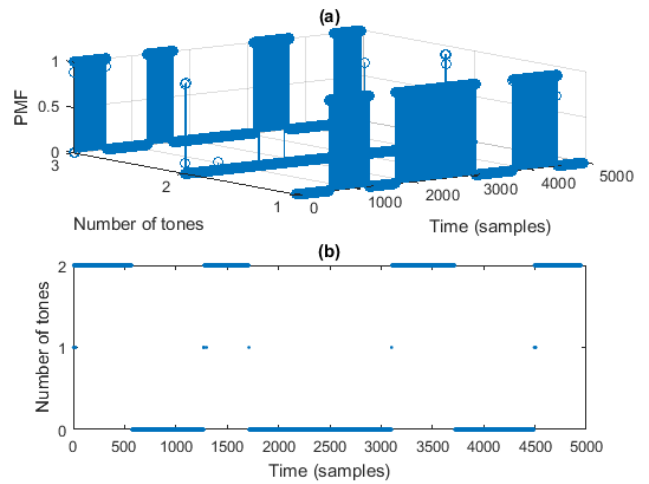


Fig. 8. Tracks of the hand-dialled DTMF signal recorded locally. (a) PMF of the number of tones. (b) Number of tones estimates.

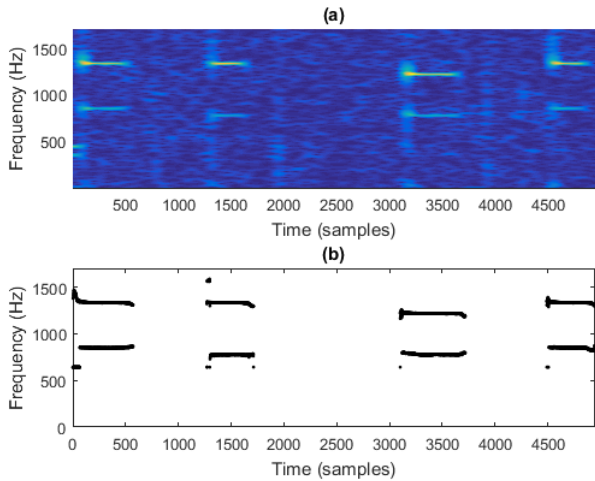


Fig. 7. (a) The spectrogram of the hand-dialled DTMF signal recorded locally. (b) Frequency estimates of the signal.

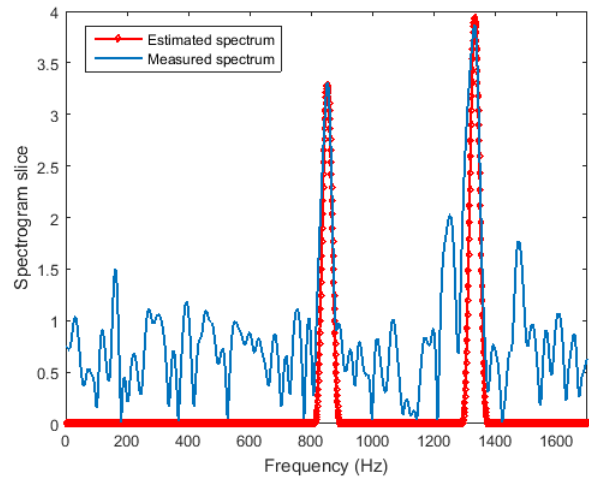


Fig. 9. A spectrogram slice of the hand-dialled DTMF signal at times step 500 with the estimated spectrum from the PF superimposed.

estimates of the PDFs are 852 and 1336 Hz, exactly the true values. However, the observation from the results is that the uncertainty of the first tone is larger than the second one. This stems from the fact that the lower frequency component from the recorded DTMF is weaker than the higher one, this leads to the larger variance in the estimated PDF.

Figs. 11(a) and (b) display two spectrograms with superimposed frequency MAP estimates for SNRs of 10 and 5 dB, respectively. As demonstrated, the frequency trajectories can track most of the DTMF tones even the noise is increased. However, the filter introduces some erroneous frequency estimates but these errors are not significant in DTMF identification since the filter can eventually provide a pair of tones correctly. This emphasizes the robustness of the filter to the noise that is present in the received signals.

Finally, we evaluate the reliability and accuracy of the filter by comparing the RMS error (RMSE) and the number of particles after adding different noise levels to the DTMF signal. The RMSE is the  $L_2$  norm averaged over  $R$  realizations and  $M$  spectrogram slides:

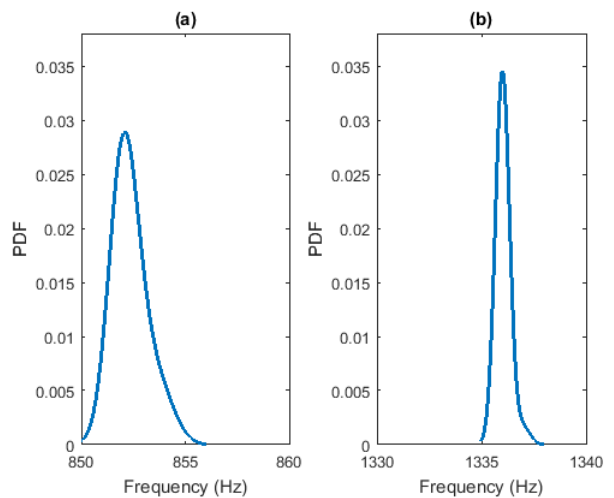


Fig. 10. The frequency PDFs of the hand-dialled DTMF signal at times slide 150 (a) first tone and (b) second tone.



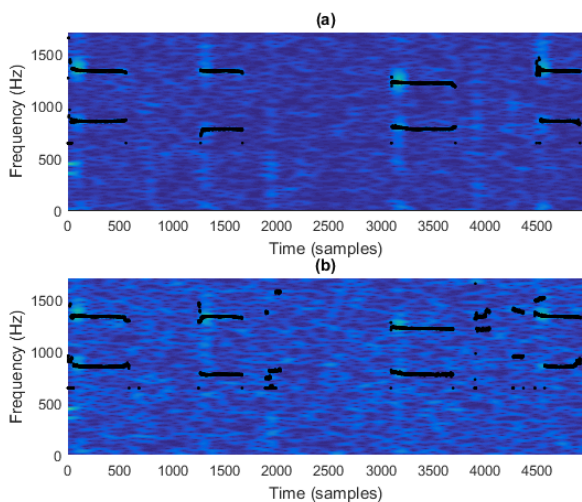


Fig. 11. Frequency tracking for two different noise levels. (a) SNR 10 dB. (b) SNR 5 dB.

$$RMSE = \sqrt{\frac{1}{RM} \sum_{n=1}^M \|\mathbf{f}'_n - \hat{\mathbf{f}}_n\|^2} \quad (23)$$

where  $\mathbf{f}'_n$  is the vector of true values of the normalized frequencies and  $\hat{\mathbf{f}}_n$  is the vector of the normalized frequency estimates at time step  $n$ . Two-hundred realizations were run for a Monte Carlo performance evaluation. The normalized quantities were obtained with the sampling frequency of 4000 Hz.

RMS results from PF implementation for identifying the modem DTMF signal, hand-dialled DTMF signal recorded over the network, hand-dialled DTMF signal recorded locally, and wideband coupling DTMF signal recorded locally are shown in Figs. 12-15, respectively. For each figure, stars indicate the RMSE for SNR of 15 dB; triangles show the error for SNR of 10 dB; circles demonstrate the error for SNR of 5 dB; lines without marker in blue, green, and red show conventional MAP errors for SNRs of 15, 10, and 5 dB, respectively. These figures confirm that the PF presents the smaller errors than those from the conventional MAP estimator. Moreover, as discussed earlier that the filter can capture the PDF in the support space comprehensively when higher number of particles is used, therefore, the results present this as had been observed in the decreasing of the RMS errors for all SNRs.

## V. CONCLUSIONS

In this paper, the Bayesian framework to address the DTMF signal identification via time-frequency representation of the signal was presented. The main goal was to identify the tones of the recorded DTMF signal in various environments. Although the signal to be tracked was corrupted by unknown noise PDFs, but DTMF signal was well governed in the frequency domain as described previously, using sophisticated Bayesian framework with a very low number of particles was sufficient to successfully extract the required information from the noisy DTMF signal. Besides, by using MMPF, it was illustrated that, for a given corrupted DTMF signal, it was achievable to estimate the tones of the signal. Number

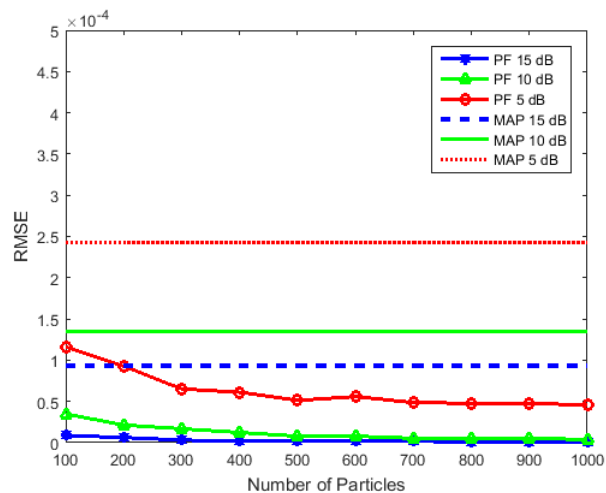


Fig. 12. PF performance for the modem DTMF signal at SNRs of 15, 10, and 5 dB: RMS errors are plotted vs the number of particles. Conventional MAP errors are also presented.

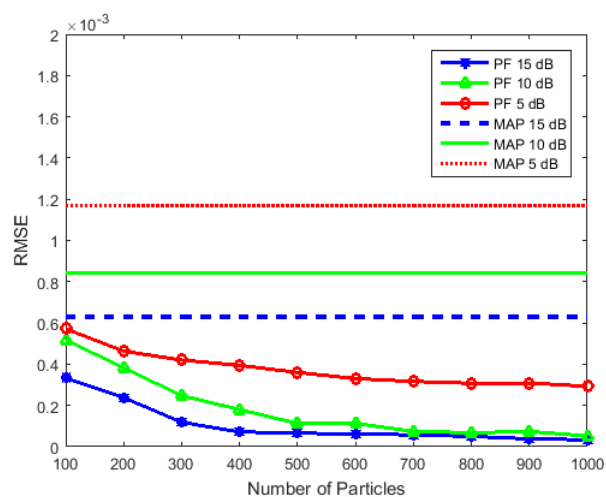


Fig. 13. PF performance for the hand-dialled DTMF signal recorded over the network at SNRs of 15, 10, and 5 dB: RMS errors are plotted vs the number of particles. Conventional MAP errors are also presented.

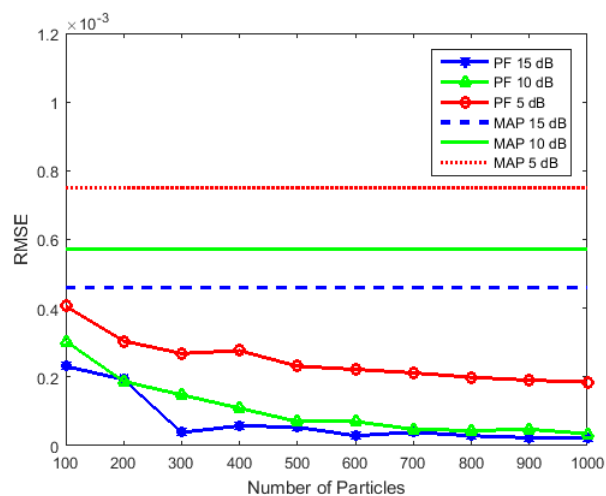


Fig. 14. PF performance for the hand-dialled DTMF signal recorded locally at SNRs of 15, 10, and 5 dB: RMS errors are plotted vs the number of particles. Conventional MAP errors are also presented.

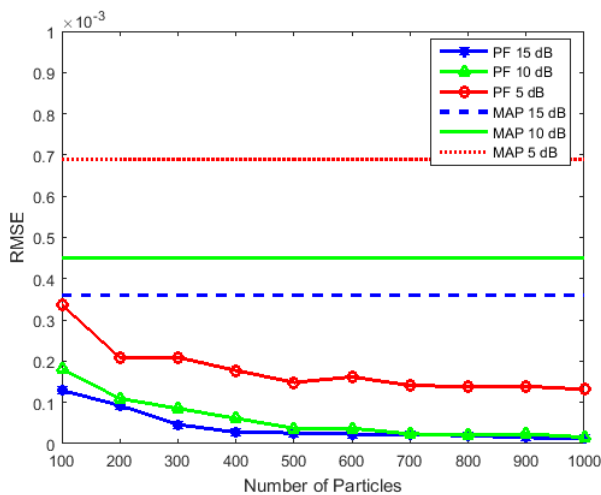


Fig. 15. PF performance for the wideband coupling DTMF signal recorded locally, at SNRs of 15, 10, and 5 dB: RMS errors are plotted vs the number of particles. Conventional MAP errors are also presented.

of tones present at a time together with the frequencies were also estimated. Moreover, some PDFs of the estimated frequencies to show how the filter accurately identifies the tones of the DTMF signal were provided. The results showed that the method exhibits excellent tracking. The performance of the approach was validated by comparing the RMS errors of the filter to the conventional MAP estimator under different noise levels, the proposed PF was found to be remarkably superior.

#### ACKNOWLEDGMENT

The author would like to thank Mae Fah Luang University for providing its facility to support this work.

#### REFERENCES

- [1] J. V. Candy, *Bayesian Signal Processing: Classical, Modern and Particle Filtering Methods*. New Jersey: John Wiley & Sons, 2009.
- [2] R. E. Kalman, "A new approach to linear filtering and prediction problems," *Transactions of the ASME - Journal of Basic Engineering*, vol. 82 (series B), pp. 35–45, 1960.
- [3] S. M. Kay, *Fundamentals of Statistical Signal Processing – Volume I: Estimation Theory*. New Jersey: Prentice-Hall, 1993.
- [4] E. A. Wan and R. van der Merve, "The unscented Kalman filter", in S. Haykin, *Kalman Filtering and Neural Networks*. New York: John Wiley & Sons, 2001.
- [5] C. Yardim, P. Gerstoft, and W. S. Hodgkiss, "Tracking of geoacoustic parameters using Kalman and particle filters," *Journal of the American Statistical Association*, vol. 125, no. 2, pp. 746–760, 2009.
- [6] Y. Bar-Shalom, X. R. Li, and T. Kirubarajan, *Estimation with Applications to Tracking and Navigation*. New York: John Wiley & Sons, 2001.
- [7] S. Julier, J. Uhlmann, and H. F. Durrant-White, "A new method for nonlinear transformation of means and covariances in filters and estimators," *IEEE Trans. Automat. Contr.*, vol. 45, pp. 477–482, 2000.
- [8] Y. Morsly and M. S. Djouadi, "Genetic algorithm combined to IMM approach for tracking highly maneuvering targets," *IAENG International Journal of Computer Science*, vol. 35, no. 1, pp. 41–46, 2008.
- [9] H. Baili, "Stochastic analysis and particle filtering of the volatility," *IAENG International Journal of Applied Mathematics*, vol. 41, no. 1, pp. 76–81, 2011.
- [10] N. Aunsri and S. Hemrungrote, "A Bayesian approach for frequency estimation using TV AR model for ocean acoustics time-series," in *Proceedings. Asia-Pacific Signal and Information Processing Association Annual Summit and Conference (APSIPA)*, 2014, pp. 1–4.
- [11] J. J. K. Ó Ruanaidh and W. J. Fitzgerald, *Numerical Bayesian Methods Applied to Signal Processing*. New York: Springer-Verlag, 1996.

- [12] B. Ristic, S. Arulampalam, and N. Gordon, *Beyond the Kalman Filter: Particle Filters for Tracking Applications*. Boston, MA: Artech House, 2004.
- [13] A. Doucet, S. Godsill, and C. Andrieu, "On sequential Monte Carlo sampling methods for Bayesian filtering," *Statistics and Computing*, vol. 10, no. 3, pp. 197–208, 2000.
- [14] A. Kong, J. S. Liu, and W. H. Wong, "Sequential imputations and Bayesian missing data problems," *J. Amer. Statist. Assoc.*, vol. 89, no. 425, pp. 278–288, 1994.
- [15] L. Dongping, "Failure prognosis with uncertain estimation based on recursive models re-sampling bootstrap and ANFIS," *IAENG International Journal of Computer Science*, vol. 43, no. 2, pp. 263–269, 2016.
- [16] N. J. Gordon, D. J. Salmond, and A. F. M. Smith, "Novel approach to nonlinear/non-Gaussian Bayesian state estimation," *IEE Proc. F, Radar and Signal Processing*, vol. 140, no. 2, pp. 107–113, 1993.
- [17] F. Gustafsson, F. Gunnarsson, N. Bergman, U. Forssell, J. Jansson, R. Karlsson, and P. J. Nordlund, "Particle filters for positioning, navigation, and tracking," *IEEE Trans. Signal Process.*, vol. 50, pp. 425–437, 2002.
- [18] O. Cappé, S. Godsill, and E. Moulines, "An overview of existing methods and recent advances in sequential Monte Carlo," *Proc. IEEE*, vol. 95, no. 5, pp. 899–924, 2007.
- [19] P. Malarvezhi and R. Kumar, "Particle filter with novel resampling algorithm: A diversity enhanced particle filter," *Wireless Personal Communications.*, vol. 84, no. 4, pp. 3171–3177, 2015.
- [20] N. Aunsri and Z.-H. Michalopoulou, "Sequential filtering for dispersion tracking and sediment sound speed inversion," *J. Acoust. Soc. Am.*, vol. 136, no. 5, pp. 2665–2674, 2014.
- [21] J. R. Larocque, J. P. Reilly, and W. Ng, "Particle filters for tracking an unknown number of sources," *IEEE Trans. Signal Processing*, vol. 50 (12), pp. 2926–2937, 2002.

**Nattapol Aunsri (M'14)** received the B.Eng. degree and M.Eng. degree in Electrical Engineering from Khon Kaen University and Chulalongkorn University, Thailand in 1999 and 2003, respectively. He obtained M.Sc. degree in Applied Mathematics and Ph.D. degree in Mathematical Sciences from New Jersey Institute of Technology, Newark, NJ, in 2008 and 2014, respectively. The author became a Member (M) of IAENG in 2014. Currently, he is a Lecturer at the School of Information Technology, Mae Fah Luang University, Chiang Rai, Thailand. His research interests include ocean acoustics, Bayesian filtering, signal processing, and mathematical and statistical modeling.